PROCEEDINGS OF SPIE

Photonics Applications in Astronomy, Communications, Industry, and High-Energy Physics Experiments 2018

Ryszard S. Romaniuk
Maciej Linczuk
Editors

3–10 June 2018
Wilga, Poland

Organized by
Institute of Electronic Systems, Faculty of Electronics and Information Technologies, Warsaw University of Technology (Poland)

Sponsored by
PSP—Photonics Society of Poland • Committee of Electronics and Telecommunications, Polish Academy of Sciences • ARIES—Accelerator Research and Innovation for European Science and Society (CERN, EU H2020) • PKOpto—Polish Committee of Optoelectronics of SEP—The Association of Polish Electrical Engineers • EuroFusion Collaboration • EuroFusion Poland

Published by
SPIE

Volume 10808

Part One of Three Parts

Proceedings of SPIE 0277-786X, V. 10808

The papers in this volume were part of the technical conference cited on the cover and title page. Papers were selected and subject to review by the editors and conference program committee. Some conference presentations may not be available for publication. Additional papers and presentation recordings may be available online in the SPIE Digital Library at SPIEDigitalLibrary.org.

The papers reflect the work and thoughts of the authors and are published herein as submitted. The publisher is not responsible for the validity of the information or for any outcomes resulting from reliance thereon.

Please use the following format to cite material from these proceedings:
Author(s), "Title of Paper," in *Photonics Applications in Astronomy, Communications, Industry, and High-Energy Physics Experiments 2018*, edited by Ryszard S. Romaniuk, Maciej Linczuk, Proceedings of SPIE Vol. 10808 (SPIE, Bellingham, WA, 2018) Seven-digit Article CID Number.

ISSN: 0277-786X
ISSN: 1996-756X (electronic)

ISBN: 9781510622036
ISBN: 9781510622043 (electronic)

Published by
SPIE
P.O. Box 10, Bellingham, Washington 98227-0010 USA
Telephone +1 360 676 3290 (Pacific Time) · Fax +1 360 647 1445
SPIE.org

Printed in the United States of America.

Publication of record for individual papers is online in the SPIE Digital Library.

SPIEDigitalLibrary.org

Paper Numbering: *Proceedings of SPIE* follow an e-First publication model. A unique citation identifier (CID) number is assigned to each article at the time of publication. Utilization of CIDs allows articles to be fully citable as soon as they are published online, and connects the same identifier to all online and print versions of the publication. SPIE uses a seven-digit CID article numbering system structured as follows:

- The first five digits correspond to the SPIE volume number.
- The last two digits indicate publication order within the volume using a Base 36 numbering system employing both numerals and letters. These two-number sets start with 00, 01, 02, 03, 04, 05, 06, 07, 08, 09, 0A, 0B … 0Z, followed by 10-1Z, 20-2Z, etc. The CID Number appears on each page of the manuscript.

THEORETICAL STUDY OF DESIGNING NEURAL ELEMENTS ON C-NEGATRONS

The C-negatron is called an electronic device and its schematic analogue, which has a negative value of the differential capacitance in a certain mode of operation. Like R-negatrons, they can be divided into static and dynamic[21]. Static C-negatrons have coulomb-volt characteristics of the N- and S-types (Fig. 1, a, b), on which there is a falling section (a, b), where the value of the differential capacitance is negative $C^{(-)} = dq/du < 0$.

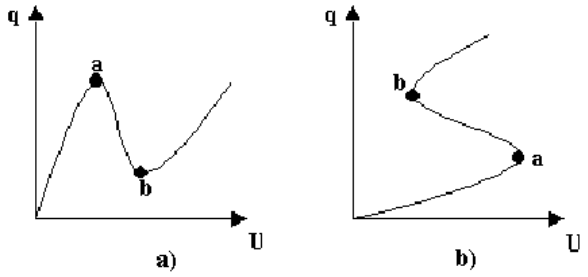

Figure 1. Coulomb-Volt characteristics of N- (a) and S-type (b) C-negatrons

In the case of using the N-type C-negatron, its simplest equivalent circuit, taking into account the load, is presented in the form shown in Fig. 2.

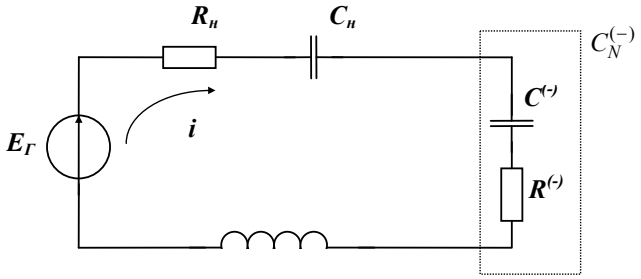

Figure 2. Equivalent scheme of loaded C-negatron of N-type. $R_н$ – total resistance of the load and internal resistance of the power supply; $C_н$ – load capacitance; L – the total inductance of the C-negatron load; $C^{(-)}$ – negative differential capacitance of C-negatron; $R^{(-)}$ – negative differential resistance of the C-negatron of the N-type

Scheme shown in Fig. 2 is described by the following Kirchhoff equations:

$$E_Г = iR + u_C + L\frac{di}{dt}, \tag{1}$$

where

$$R = R_н + R^{(-)}; \tag{2}$$

$$u_C = u_{C_н} + u_{C^{(-)}};$$

$$i = C\frac{du_C}{dt}; \tag{3}$$

$$C = \frac{C_н \cdot C^{(-)}}{C_н + C^{(-)}}. \tag{4}$$

Taking into account (3) - (4), we write the equation (1) in the following form:

$$\frac{d^2u_C}{dt^2}+\frac{R_н+R^{(-)}}{L}\frac{du_C}{dt}+\frac{u_C}{L\dfrac{C_н\cdot C^{(-)}}{C_н+C^{(-)}}}=\frac{E_г}{L\dfrac{C_н\cdot C^{(-)}}{C_н+C^{(-)}}}. \tag{5}$$

Taking into account (5), we assume that $C^{(-)}$ and $R^{(-)}$ are linear elements that are valid for small signal. In this case, the characteristic equation for (5) has the form

$$\lambda^2+\sigma\lambda+p=0, \tag{6}$$

where

$$\sigma=\frac{R_н+R^{(-)}}{L}, \tag{7}$$

$$p=\frac{C_н+C^{(-)}}{LC_нC^{(-)}}, \tag{8}$$

$$\lambda_{1,2}=-\frac{\sigma}{2}\pm\sqrt{\frac{\sigma^2}{4}-p}, \tag{9}$$

$\lambda_{1,2}$ – the roots of the characteristic equation.

The solution of the inhomogeneous differential equation (5) is look like

$$u_C=Ae^{\lambda_1 t}+Be^{\lambda_2 t}+E_г. \tag{10}$$

Voltage on the negative capacitance $C^{(-)}$

$$u_{C^{(-)}}=\frac{u_CC_н}{C^{(-)}+C_н}.$$

To analyze the stability of the scheme depicted in Fig. 2, it is necessary to determine the states of equilibrium and their stability. In a state of equilibrium, the phase velocities of the current and the voltage are equal to zero, i.e.

$$\frac{di}{dt}=0 \text{ i } \frac{du}{dt}=0. \tag{11}$$

Substituting expression (11) in (1) we obtain

$$E_г=u_C \text{ or } u_{C^{(-)}}=E_г-u_{C_н}.$$

Since $u_{C_н}=\dfrac{q_{C_н}}{C_н}$ and when the capacitors are connected in series, their charges are equal, i.e. $q_{C^{(-)}}=q_{C_н}$, then the equation of the loading line can be written in the form

$$q(u)=(E_г-u)C_н.$$

Thus, the states of equilibrium are points of intersection of the coulomb-volt character of the N-type C-negatron with the loading line. Such crossing points can be either one or three (Fig. 3). In case if $\left|C^{(-)}\right|>C_н$, the load line (Fig. 3a) intersects the coulomb-volt characteristic at three points (three states of equilibrium). If $\left|C^{(-)}\right|<C_н$, then there is only one equilibrium state (Fig. 3b).

The stability of these points can be judged by the roots of the characteristic equation λ_1 and λ_2. If λ_1 and λ_2 are real, then from (10) it is clear that with $\lambda_{1,2} < 0$ any initial deviation in the system fades out under exponential law, and if $\lambda_{1,2} > 0$ – increases. If the roots of the characteristic equation are complex ($\lambda_{1,2} = a + jb$), then the system may have sinusoidal oscillations, and if $a > 0$ the fluctuations are increased, and if $a < 0$ – decreased.

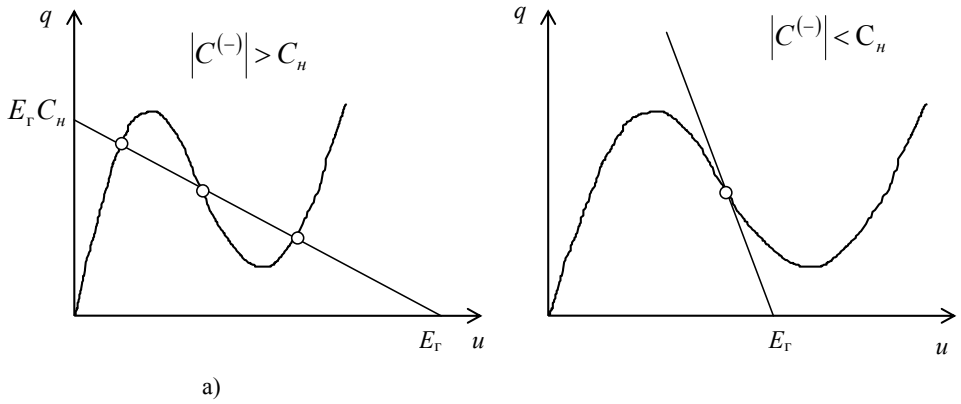

a)

b)

Figure 3. Possible equilibrium states of N-type C-negatrons

Consequently, the state of the system is stable if the real parts of the roots of the characteristic equation (6) are negative. For this purpose, by the Raus-Hurwitz theorem for systems of the second order, it is sufficient that two conditions be fulfilled simultaneously[21]:

$$\sigma > 0; \quad p > 0. \tag{12}$$

Coefficients σ and p depend on the scheme parameters. From (7) and (8) it is clear that for a constant L the fulfillment or non-fulfillment of conditions (12) depends on $R_н$, $C_н$, $R^{(-)}$ and $C^{(-)}$. Differential negative capacitance $C^{(-)}$ and negative resistance $R^{(-)}$ of the C-negatron are changed with the bias voltage change. Therefore, when changing the resistance and capacitance of the load or the bias voltage on the N-type C-negatron, the mode of operation of the circuit is changed. We consider only the interval of the bias voltage in which the differential capacitance and the resistance of the C-negatron are negative ($C^{(-)} < 0$, $R^{(-)} < 0$), that is, only the states of equilibrium on the segment of the negative capacitance of the coulomb-volt characteristic of the N-type C-negatron.

Let us consider the equilibrium states of the scheme at different ratios σ and p, that is, depends on the ratio of the quantities $C_н$, $R_н$, $C^{(-)}$, $R^{(-)}$. From expressions (7) - (9) it is clear that four boundary conditions can be written:

1) $$p = \frac{C_н + C^{(-)}}{LC_н C^{(-)}} = 0, \tag{13}$$

if $C_н = -C^{(-)}$.

2) $$\sigma = \frac{R_н + R^{(-)}}{L} = 0, \tag{14}$$

if $R_н = -R^{(-)}$.

3) $$\frac{\sigma^2}{4} - p = 0, \tag{15}$$

if $C_н = \dfrac{4L}{\left(R_н + R^{(-)}\right)^2 - 4L/C^{(-)}}$.

4) $$\frac{\sigma^2}{4} - p = 0, \tag{16}$$

$$\text{if } R_{н_{1,2}} = -R^{(-)} \pm 2\sqrt{\frac{L\left(C_н + C^{(-)}\right)}{C_н C^{(-)}}}.$$

For boundary conditions (15) and (16) there is a solution only when $p \geq 0$.

Since the fulfillment or non-fulfillment of the stability conditions (12) depends on the correlation of two pairs of parameters: $C_н$, $C^{(-)}$ and $R_н$, $R^{(-)}$, then the stability diagrams is also reflected as the two planes of the parameters.

Area *I* in the plane of the parameters $C^{(-)}$ $C_н$ corresponds to two regions in the plane of the parameters $R^{(-)}$ $R_н$ – *Ia* and *Ib*. Area *II* in the plane of the parameters $C^{(-)}$ $C_н$ corresponds to two areas (*IIa* and *IIb*) in the plane of the parameters $R^{(-)}$ $R_н$. Area *III* in the plane of the parameters $C^{(-)}$ $C_н$ corresponds to two areas (*IIIa* and *IIIb*) in the plane of the parameters $R^{(-)}$ $R_н$. Thus, in the stability diagram of the C-negatron of the N-type, there are six different regions (*Ia*, *Ib*, *IIa*, *IIb*, *IIIa*, *IIIb*), which determine the mode of operation of C-negatron.

Region Ia.

$$\sigma > 0 \text{ or } R_н > \left|R^{(-)}\right|,$$

$$p < 0 \text{ or } C_н > \left|C^{(-)}\right|,$$

$$\sqrt{\frac{\sigma^2}{4} - p} > \frac{\sigma}{2}.$$

The roots of the characteristic equation λ_1 and λ_2 – real numbers, and moreover $\lambda_1 > 0$, and $\lambda_2 < 0$. Consequently, the first term of equation (10) grows exponentially, and the second one - decreases. Because in this area $C_н > \left|C^{(-)}\right|$, then only one equilibrium state is possible (see Fig. 3). Since one of the roots of the characteristic equation is positive, then the only one equilibrium state is unstable. The scheme works in the mode of generating relaxation oscillations.

Region Ib

$$\sigma < 0 \text{ or } R_н < \left|R^{(-)}\right|,$$

$$p < 0 \text{ or } C_н > \left|C^{(-)}\right|,$$

$$\frac{\sigma^2}{4} - p > 0.$$

The roots of the characteristic equation λ_1 and λ_2 – real numbers, and moreover $\lambda_1 > 0$, and $\lambda_2 < 0$. Consequently, the first term of equation (10) grows exponentially, and the second one - decreases. Because in this area $C_н > \left|C^{(-)}\right|$, then only one equilibrium state is possible. Taking into account that one of the roots of the characteristic equation is positive, and then the only state of equilibrium is unstable. The scheme works in the mode of generating relaxation oscillations.

Region IIa

$$\sigma > 0 \text{ or } R_н > \left|R^{(-)}\right|,$$

$$p > 0 \text{ or } C_н < \left|C^{(-)}\right|,$$

$$\frac{\sigma^2}{4} - p > 0 \ .$$

The roots of the characteristic equation λ_1 and λ_2 – real and negative numbers. Both exponential members of the equation (10) decrease over time. Because $C_н < \left|C^{(-)}\right|$, then three states of equilibrium are possible, and the state of equilibrium is stable in the section of negative capacitance. The circuit can work as a nonlinear element (detector, converter, mixer, and limiter) with amplification.

Region IIb

$$\sigma < 0 \text{ or } C_н < \left|C^{(-)}\right|,$$

$$p > 0 \text{ or } C_н < \left|C^{(-)}\right|,$$

$$\frac{\sigma^2}{4} - p > 0 \ .$$

Roots λ_1 and λ_2 – real positive numbers. The first two members of the equation (10) increase over time according to the exponential law. Since $C_н < \left|C^{(-)}\right|$, then three states of equilibrium are possible, and the state of equilibrium in the area of the negative capacitance is unstable. Two other states of equilibrium is stable, because $C^{(-)} > 0$ and both coefficients σ and p are positive. So, in the area *IIb* the circuit works in the switching mode.

Region IIIa

$$\sigma > 0 \text{ or } R_н > \left|R^{(-)}\right|,$$

$$p > 0 \text{ or } C_н < \left|C^{(-)}\right|,$$

$$\frac{\sigma^2}{4} - p < 0 \ .$$

Roots λ_1 and λ_2 – complex numbers with negative real part. Consequently, in accordance with (10), the system has an oscillating process that fades out according to the exponential law. Because $C_н < \left|C^{(-)}\right|$, then three states of equilibrium are possible, and the state of equilibrium in the area of negative capacitance is unstable. The circuit works in the amplification mode.

Region IIIb

$$\sigma < 0 \text{ or } R_н < \left|R^{(-)}\right|,$$

$$p > 0 \text{ or } C_н < \left|C^{(-)}\right|,$$

$$\frac{\sigma^2}{4} - p < 0 \ .$$

Roots λ_1 and λ_2 – complex numbers with a positive real part. Consequently, the first two terms in equation (2.17) describe a periodic process whose amplitude increases in exponential law. Since $C_н < \left|C^{(-)}\right|$, then three states of equilibrium are possible, and the state of equilibrium in the area of the negative capacity is unstable. The circuit works in the switching mode.

Thus, the mode of operation of the scheme with the C-negatron of the N-type depends on the capacitance and the resistance of the load, the values of the negative capacitance and the negative resistance of the negatron. Choosing the appropriate capacity and the resistance of the load and the bias voltage, which determines the values $C^{(-)}$ and $R^{(-)}$,you can get such modes of work:

a) generation of relaxation oscillations - areas *Ia* and *Ib*;

b) detection (mixing, limitation) with amplification is the area *IIa*;

c) switching - areas *IIb* and *IIIb*;

d) amplification - area *IIIa*.

The presence of a negative capacitance makes the C-negatron a potentially unstable and multifunctional device. With the correct choice of load parameters, the scheme on the C negatron will operate in the switching mode[21], and the C-negatron will act as a threshold element. So with $C_{Load} < \left(C^{(-)}\right)$ the load line crosses the coulomb-volt characteristic of the N-type C-negatron as shown in Fig. 4. When supplying an input current $i(t)$, the charge $q(t)$ on the C-negatron will increase, and the position of the working point will move from position 1 to 2. In this case, the function of integration of the input current signal will be provided, since $q(t) = \int_0^t i(t)dt$. When reaching the threshold value of the charge Q_{th} the switching of the C-negatron will take place, and the operating point instantly moves from position 3 to position 4, and the voltage on the C-negatron will jump from U_{th} to U_{high}.

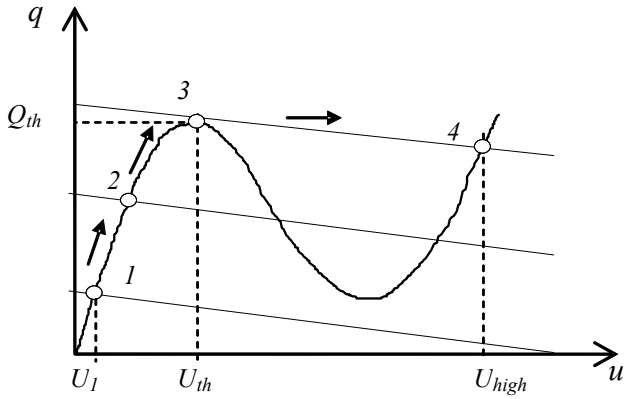

Figure 4. The load line and equilibrium positions of the N-type C-negatron

Similarly, but with $C_{Load} > \left|C^{(-)}\right|$ the S-type C-negatron will work in switching mode[21-35] and perform the functions of integrating the input current and the function of the threshold element.

Proceeding from the above-mentioned principle of the threshold element, the scheme of the optoelectronic neuron element based on the N-type C-negatron is shown in Fig. 5. In the scheme: C_{load} – the load capacitance - determines the slope of the load line; C(-)N – the N-type C-negatron - performs the integration of input current signals and the threshold activation function; VD1-VD3 excitation and VD4 inhibition photodiodes provide conversion of input optical signals

into photocurrents. This scheme has optical inputs (and the number of optical inputs is quite easy to enlarge by adding new photodiodes parallel to the circuit, or by feeding several optical streams to one photodiode) and the potential voltage output.

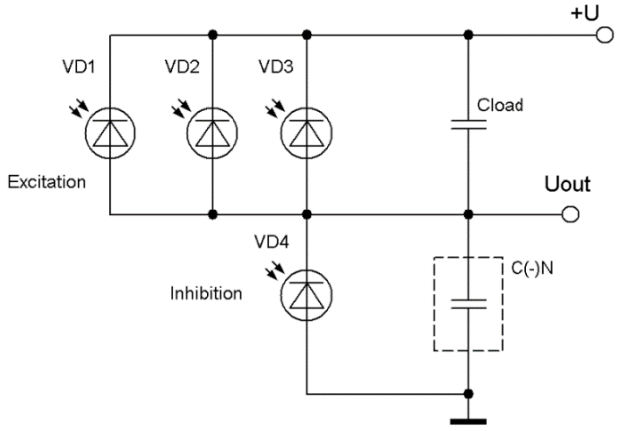

Figure 5. Optoelectronic neuron on the N-type C-negatron

The voltage at the output will be determined by the expressions:

$$U_{out} \le U_{th} \text{ if } Q = \int_0^t i_\Sigma(t)\,dt \le Q_{th} \text{ where } i_\Sigma = \sum_{j=1}^{n} i_j - \sum_{j=1}^{m} i_j ,$$

$$U_{out} \ge U_{high} \text{ if } Q = \int_0^t i_\Sigma(t)\,dt > Q_{th} .$$

Thus, this scheme carries out a spatial algebraic summation of input signals from photodiodes: the total input current $i_\Sigma = \sum_{j=1}^{n} i_j - \sum_{j=1}^{m} i_j$, where n - the number of photodiodes of excitement, m - the number of photodiodes of inhibition; and the time integration of the input signals: the charge of the C-negatron $Q = \int_0^t i_\Sigma(t)\,dt$.

COMPUTER SIMULATION

We conduct a computer simulation of the proposed neuron with the Micro-Cap 9 program. This program is convenient for this use, since it has the ability to specify a non-linear coulomb-volt characteristic of a capacitance.

The conducted literature analysis has shown that at present, the effect of negative capacitance is observed in different semiconductor structures in different conditions (homogeneous semiconductors[12], homostructures[13], heterostructures[15], metal-semiconductor type structures[14], amorphous semiconductor films[16]) and in other charge electrified structures[17]. Non-linear coulomb-volt characteristic having a section of negative differential capacitance can be obtained in film capacitors with a ferroelectric dielectric[20]. Such physical C-negatrons are compatible with CMOS-technology for the production of integrated circuits. However, physical C-negatrons are still at the research stage and there is no detailed experimental data that would allow us to develop a mathematical model for these C-negatrons. Therefore, for computer simulations, let us determine certain parameters of the C-negatron, which will allow us to check the efficiency of the circuit and to investigate its operation in different modes.

For simulation we use the C-negatron of the N-type with the coulomb-volt characteristic (Fig. 6a) which we describe by the polynomial of the 3-rd order:

$$q(u) = 8{,}8 \cdot 10^{-9} \cdot u - 4{,}35 \cdot 10^{-9} \cdot u^2 + 0{,}55 \cdot 10^{-9} \cdot u^3 .$$

For this characteristic, the threshold charge value $Q_{th} = 530$ pC, the threshold voltage $U_{th} = 1.4$ V, the negative differential capacitance is observed in the range of voltages $U = 1.4 \div 3.9$ V, the maximum value of the negative capacitance is observed at the voltage U_C=2.65 V, and it equals $C_{max}^{(-)}$ = -267pF (Fig. 6, b). For operation of the C-negatron N-type in the switching mode it is necessary $C_{Load} < \left(C^{(-)}\right)$ so we choose the value of the load capacitance 10pF, and the value of the high-level voltage $U_{high} \approx 5$ V (Fig. 6, a).

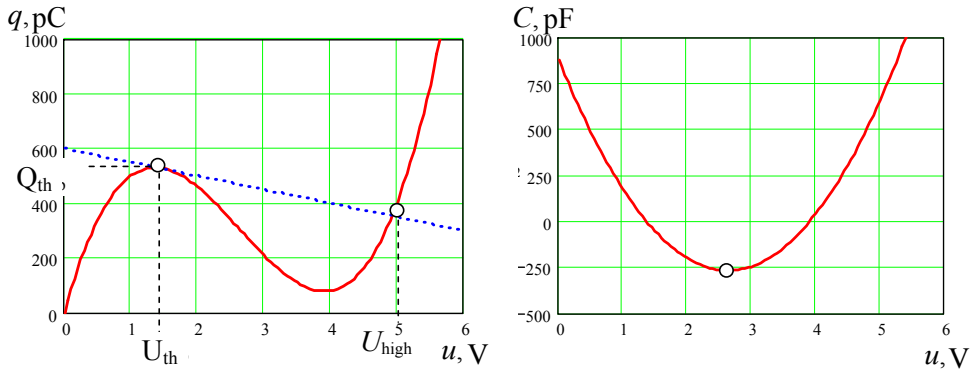

a) b)

Figure 6. Coulomb-Volt (a) and Volt-Farad (b) characteristics of the N-type C-negatron

Fig. 7 shows a schematic diagram for simulation in the Micro-Cap 9 program. Photodiodes are replaced by current generators I1 to I4, and R1 represents the impedance of the dielectric of the load capacitor C1, the charge of the C-negatron CN is given by the expression Q (CN). Fig. 8 shows the timing diagram of the neuron. Input current I1 = 5mA, the charge of the C-negatron Q (CN) is increased by charging the capacitance, and at the instant of time 90.6ns the charge reaches the threshold $Q_{th} = 530$pQ, and the output voltage jumps from $U_{th} = 1.4$V to U_{high}=5V. The switching time, according to the simulation results, is much less than 1ps. However, the scheme does not take into account parasitic elements, which in practice will worsen the speed of the scheme. To discharge the circuit into the initial state, it is necessary to apply a current pulse to the inhibition input, it will discharge the capacitance of the C-negatron and the output voltage will be about 0 V.

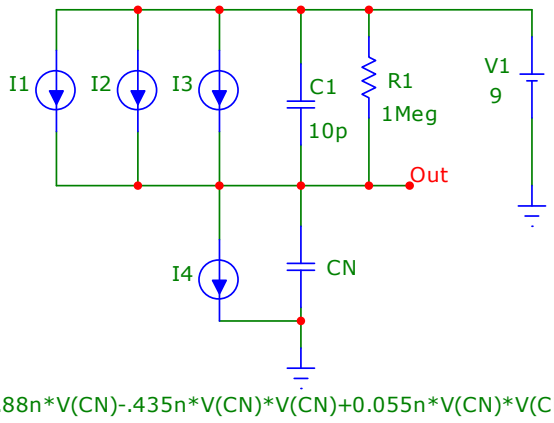

Figure 7 - Neuron on C-negatron scheme for simulation with Micro-Cap 9.

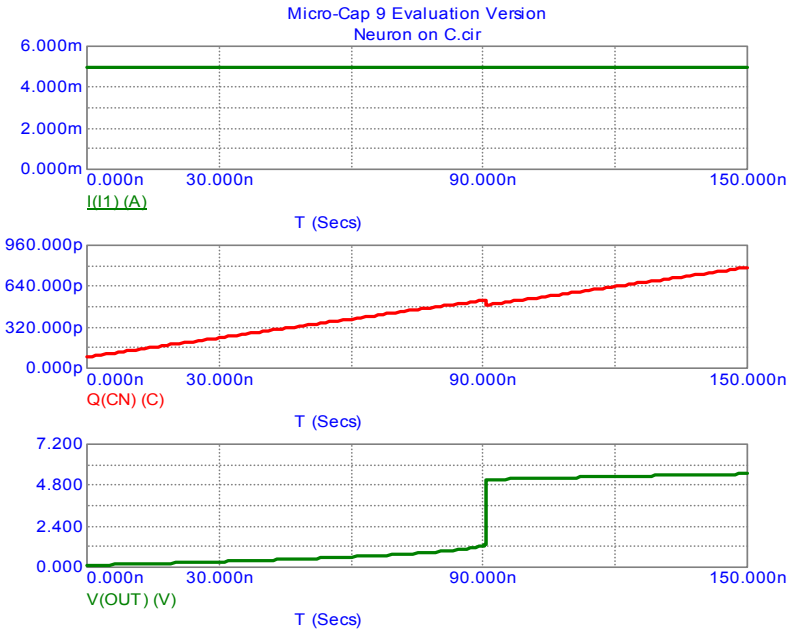

Figure 8 - Time charts of the neuron: (I1) - the input photocurrent of the excitation signal;Q (CN) - the C-negatron charge; V (OUT) - voltage at the neuron output

Fig. 9 shows the time diagram of the neuron on C-negatron operation for pulsed input signals on the excitation inputs I1, I2, and3. Each of these signals charges the capacitance of the C-negatron, but the charge of individual signals is not enough to transfer the circuit into the high state. The scheme performs the integration of input signals, and when the total charge of all three signals exceeds the threshold charge of the C-negatron, there is the circuit switching. Thus, the neuron can perform the logical function of "AND" of binary logic. To transfer the circuit to a low state on the inhibition input I4, a discharge current pulse is fed.

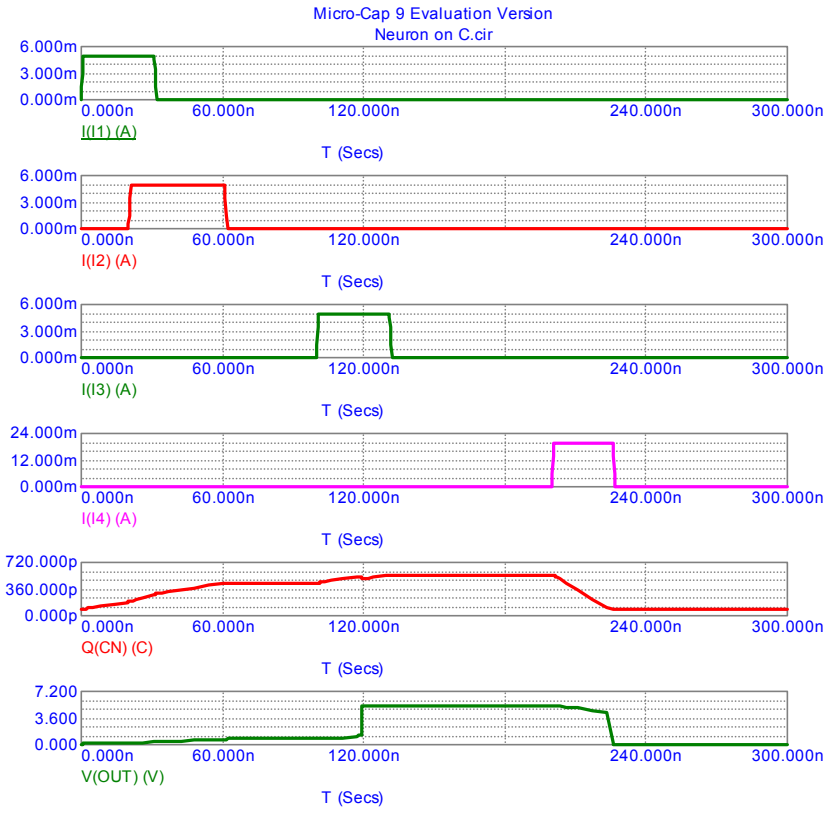

Figure 9 - Time charts of the neuron on the C-negatron operation: I (I1), I (I2), I (I3) - input photocurrents of excitation signals; I(I4) - the photocurrent of the inhibition signal (the signal of a discharge); Q (CN) - charge of the C-negatron; V(OUT) - voltage at the output of the neuron

CONCLUSIONS

1. The proposed optoelectronic neuron element comprises: photodiode(s) of excitation, photodiode(s) of inhibition, load capacitor, C-negatron of N-type; and implements the following basic functions of the neuron: spatial and temporal integration (algebraic summation) of the input signals; threshold activation function. At the output of the neuron there is a high-level voltage if the total input charge exceeds a certain threshold, which is determined by the coulomb-volt characteristic of the N-type C-negatron.
2. This neuron can perform logic functions "AND", "OR", "NOT" of Boolean logic, to work as an RS-trigger, memory element, pulse width and phase-pulse modulators, to perform neuronal logic functions over time impulse-coded input signals.
3. The advantage of neural elements on C-negatrons is: high speed (the switching time is less than 1ps); circuit simplicity (the functions of integration and activation are performed by one C-negatron); technological simplicity (C-negatron can be a film condenser with a ferroelectric dielectric, which is compatible with well-developed CMOS-technology for the manufacture of integrated circuits); the ability to amplify the voltage; low power consumption (capacitance does not consume active power); the C-negatron is controlled by a charge, which allows it to work not with currents and voltages, but directly with the charge.

REFERENCES

[1] Galushkin, A. I., [Neurocomputers], Moscow: IPRHP, (2000).
[2] Khaikin, S., [Neural networks: full course. Neural Networks: A Comprehensive Foundation], Moscow Williams, (2006).

[3] Bernstein, K. and Rohrer, N. J., Pat. 6501294 B2 USA, MKI H03K 19/23. Neuron circuit /, (USA). - No. 09/842736; (2002).
[4] Sthefe, V. I., Komarovsky, K. F. and Fursin, G. I., [Neuron and other functional circuits with bundled communication], Moscow Radio and Communications, (1981).
[5] Krasilenko, V. G., Nikolsky, A. I. and Lazarev, A. A., "Optoelectronic triggers based on λ-devices as advanced components for optical computing arrays," Proc. SPIE 5104, (2003).
[6] Bardachenko, V. F, Kolesnitsky, O. K. and Vasiletsky, S. A., [Timer Neural Elements and Structures], UNIVERSUM, Vinnytsia, (2004).
[7] Filinyuk, N. A. and Lazarev, A. A., "Short historical review of development of scientific branch ”negatronics”," AEU - International Journal of Electronics and Communications, 68 (2), 172-177 (2014).
[8] Krasilenko, V. G., Nikolskyy, A. I., Lazarev, A. A., Krasilenko, O. V. and Krasilenko, I. A., "Simulation of continuously logical ADC (CL ADC) of photocurrents as a basic cell of image processor and multichannel optical sensor systems," Proc. SPIE 8774, (2013).
[9] Krasilenko, V. G., Lazarev, A. A., Grabovlyak, S. K. and Nikitovich, D. V., "Using a multi-port architecture of neural-net associative memory based on the equivalency paradigm for parallel cluster image analysis and self-learning," Proc. SPIE 8662, (2013).
[10] Bilynsky, Y., Horodetska, O. and Ratushny, P., "Prospect for the Use of New Method of Digital Processing of Medical Images," 13th International Conference on Modern Problems of Radio Engineering, Telecommunications and Computer Science, Modern problems of radio electronics, telecommunications, computer engineering (TCSET), 780 - 784, (2016).
[11] Mykhalevskiy, D., Vasylkivskyi, N. and Horodetska, O., "Development of a mathematical model for estimating signal strength at the input of the 802.11 standard receiver, " Eastern-European Journal of Enterprise Technologies 6/9 (90), 38-43, (2017).
[12] Penin, N. A., "Negative capacitance in semiconductor structures," FTP T.30(4), 626-634 (1996).
[13] Ershov, M., Liu, H. C., Li, L., Buchanan, M., Wasilevski, Z. R. and Jonscher, A. K., "Negative capacitance effect in semiconductor devices," IEEE Trans. On Electron Devices 45(10), 2196-2203 (1998).
[14] Wu, X., Yang, E. S. and Evans, H. L., "Negative capacitance at metal-semiconductor interfaces," J. Apll. Phys 68(6), 2845-2848 (1990).
[15] Boltaev, A. P., Burbaev, T. M., Kurbatov, V. A., Rzayev, M. M., Penin, N. A. and Sibel'din, N. N., "Effects of charge accumulation and negative capacitance in silicon-based heterostructures, " Izvestiya Akademii Nauk. Physical 2, 312-318 (1999).
[16] Abdulayev, A. G, Vethov, V. A, Kasimov, F. D. and others. "Negative capacity in locally grown films of polycrystalline silicon," Electronic technology Ser. 3. Microelectronics T. N. 4, 21-25 (1985).
[17] Partenskii, M. B., Dorman, V. L. and Jordan, P. C. "The question of negative capacitance and its relation to instabilities and phase transitions at electrified interfaces,” Int. Rev. Phys. Chem 11(153), 153-181 (1996).
[18] Anup, P. Jose, Kenneth L. Shepard, "Distributed Loss-Compensation Techniques for Energy-Efficient Low-Latency On-Chip Communication," IEEE Journal of Solid-State Circuits 42(6), 1415-1424 (2007).
[19] Kolev Svilen, Delacressonniere Bruno, Gautier Jean-Luc. "Using a negative capacitance to increase the tuning range of a varactor diode in MMIC technology," IEEE Trans. on Microwave Theory and Techniques 49(12), 2425-2430 (2007).
[20] Zhirnov V. V. and Cavin, R. K., "Negative capacitance to the rescue?," Nature Nanotechnology 3, 77-78 (2008).
[21] Lazarev, A., [L-, C-negatrons in Electronic Circuits], LAP LAMBERT Academic Publishing, (2017).
[22] Vedmitskyi, Y. G., Kukharchuk, V. V. and Hraniak, V. F., "New non-system physical quantities for vibration monitoring of transient processes at hydropower facilities, integral vibratory accelerations," Przeglad Elektrotechniczny 93(3), 69-72 (2017)
[23] Kukharchuk, V. V., Kazyv, S. S. and Bykovsky, S. A., "Discrete wavelet transformation in spectral analysis of vibration processes at hydropower units," Przeglad Elektrotechniczny 93(5), 65-68 (2017)
[24] Kukharchuk V. V., Hraniak V. F., Vedmitskyi Y. G., Bogachuk, V. V. and etc. "Noncontact method of temperature measurement based on the phenomenon of the luminophor temperature decreasing", Proc. SPIE 10031, (2016).
[25] Kukharchuk, V. V., Bogachuk, V. V., Hraniak, V. F., Wójcik, W., Suleimenov, B. and Karnakova, G., "Method of magneto-elastic control of mechanic rigidity in assemblies of hydropower units", Proc. SPIE 10445, (2017).

[26] Osadchuk, A., Osadchuk I., Smolarz, A. and Kussambayeva, N. "Pressure transducer of the on the basis of reactive properties of transistor structure with negative resistance," Proc. SPIE 9816, (2015).
[27] Osadchuk, O., Osadchuk V. and Osadchuk I., "The Generator of Superhigh Frequencies on the Basis Silicon Germanium Heterojunction Bipolar Transistors," 13th International Conference on Modern Problems of Radio Engineering, Telecommunications and Computer Science (TCSET), 336-338 (2016).
[28] Semenov, A. O., Osadchuk, A. V., Osadchuk, I. A., Koval, K. O. and Prytula, M. O., "The chaos oscillator with inertial non-linearity based on a transistor structure with negative resistance," Proceedings of the International Conference Micro/Nanotechnologies and Electron Devices (EDM),17th International Conference of Young Specialists.(2016).
[29] Tarnovskii, N. G., Osadchuk, V. S. and Osadchuk, A. V., "Modeling of the gate junction in GaAs MESFETs," Russian Microelectronics 29(4), 279–283 (2000)
[30] Azarov, O., Chernyak, O. and etc., "High-speed counters in Fibonacci numerical system," Proc. SPIE 10445, (2017)
[31] Azarov, O. D., Troianovska, T. I. and etc., "Quality of content delivery in computer specialists training system," Proc. SPIE 10445,(2017).
[32] Azarov, O. D., Krupelnitskyi L. V. and Komada, P., "AD systems for processing of low frequency signals based on self calibrate ADC and DAC with weight redundancy," Przegląd Elektrotechniczny 93(5), 125-128 (2017).
[33] Azarov, O. D., Dudnyk, O. V., Kaduk, O. V., Smolarz, A. and Burlibay, A., "Method of correcting of the tracking ADC with weight redundancy conversion characteristic," Proc. SPIE 9816, (2015).
[34] Azarov, O. D., Murashchenko, O. G., Chernyak, O. I., Smolarz, A. and Kashaganova, G., "Method of glitch reduction in DAC with weight redundancy," Proc. SPIE 9816, (2015).
[35] Lazarev, A. A., Voytsekhovskaya, E. V. and Zyska, T., "Research of a filter on the parallel contour on L-, C-negatrons," Proc. SPIE 10445, (2017).

Image Steganography for Increasing Security of OTP Authentication

Aldrin Wilfred Arokiasamy[a] and Władysław Skarbek[a]

[a]Warsaw University of Technology, Dept. of Electronics and Information Technology, Nowowiejska 15/19, 00-665, Warsaw, Poland

ABSTRACT

Verification of customer in web based banking system is a significant issue these days where exchanges are done utilizing uncertain Internet. The advanced communication medium is particularly experiencing a lot of threats. Picture identification and One Time Password (OTP) were commonly used to authenticate the customer over many banking systems. In most of the cases they were sent separately which is vulnerable in many cases. To solve this issue, this paper aims to give a method using both the image with hidden customer information and the OTP which is sent as SMS to user mobile. Personal Identification Number (PIN) provided by the bank at the time of registration is used to activate the process of image steganography and sending OTP to the user. The user has to know the image which was opted at the time of registration. The OTP has to be entered in a virtual keypad that has random keys to avoid key logging, used for decrypting the information hidden in the image. The image, the hidden information should match with the information in the database, thus providing the session for the customer.

Keywords: One Time Password, Cryptography, Image Steganography, Banking Security, User-Authentication, Information Security, Security Principles, Internet

1. INTRODUCTION

The Internet is termed to be beneficial to the society. It has an impact on providing various services at ease and comfort. There was an increase in the number of people who were using Internet for their financial exchanges and to administrate their online banking account, as it was providing a lot of advantages. Concerning over the Internet, there were notably many security and potential threats in terms related to transactions. In an anonymous network, there were many methods of authentication. To get the access to the users confidential data, the user has to prove their identity. The root level of confirmation is the password which was altered only when required. The password used here is static which were easy to remember and utilized at every moment when the user requires a login. The weak passwords are simple to guess by an unauthorized person and are prone to eavesdropping, dictionary brute force attack, and birth date attacks. The One-Time passwords (OTP) were introduced to decrease the threat dealing with these weak static passwords. These exhibits different level of verification which has to be proved so that the user can proceed with financial or business exchanges. The personal information of the user including his mobile number registered with the bank was required when the user opts for online transaction session. The mobile number is used to verify using SMS and to initiate the process of exchanges. The SMS that is the OTP is valid only for specific time and session, which gives the second level of confirmation and the session is provided according to the validation.

2. INFORMATION SECURITY

The widely used methods for information security were Cryptography and Steganography. The art of secret writing the mainly follows confusion and diffusion of information into cipher text is called cryptography. The art of hiding secret information under a cover object is called steganography. An email, SMS, an image, rough text may be used as a cover object. Image steganography is a method of hiding potential information inside

Further author information: (Send correspondence to W.S.)
W.S.: E-mail: wskarbek@ire.pw.edu.pl

Photonics Applications in Astronomy, Communications, Industry, and High-Energy Physics Experiments 2018, edited by Ryszard S. Romaniuk, Maciej Linczuk, Proc. of SPIE Vol. 10808, 108080Q
 · doi: 10.1117/12.2501545